

Quantum phase transition in quantum dot trimers

Andrew K. Mitchell, Thomas F. Jarrold, and David E. Logan

Department of Chemistry, Physical and Theoretical Chemistry, Oxford University, South Parks Road, Oxford OX1 3QZ, United Kingdom

(Received 17 January 2009; published 26 February 2009)

We investigate a system of three tunnel-coupled semiconductor quantum dots in a triangular geometry, one of which is connected to a metallic lead, in the regime where each dot is essentially singly occupied. Both ferromagnetic and antiferromagnetic spin- $\frac{1}{2}$ Kondo regimes, separated by a quantum phase transition, are shown to arise on tuning the interdot tunnel couplings and should be accessible experimentally. Even in the ferromagnetically-coupled local moment phase, the Kondo effect emerges in the vicinity of the transition at finite temperatures. Physical arguments and numerical renormalization group techniques are used to obtain a detailed understanding of the problem.

DOI: 10.1103/PhysRevB.79.085124

PACS number(s): 73.63.Kv, 71.27.+a, 72.15.Qm

I. INTRODUCTION

Nanofabrication techniques developed over the last decade,^{1–8} together with atomic-scale manipulation using scanning tunneling microscopy,^{9,10} have sparked intense interest in novel mesoscopic devices where strong electron correlation and many-body effects play a central role.¹¹ The classic spin- $\frac{1}{2}$ Kondo effect¹²—in which a single spin is screened by antiferromagnetic coupling to conduction electrons in an attached metallic lead—has been observed in odd-electron semiconductor quantum dots, single molecule dots, and adatoms on metallic surfaces,¹¹ although its ferromagnetic counterpart, where the spin remains asymptotically free, has yet to be reported experimentally. In *coupled* dot devices—the “molecular” analogue of single quantum dots viewed as artificial atoms²—exquisite experimental control is now available over geometry, capacitance, and tunnel-couplings of the dots.^{5,6} Both spin and internal, orbital degrees of freedom—and hence the interplay between the two—are important in such systems. This leads to greater diversity in potentially observable correlated electron behavior on coupling to metallic leads, as evident from a wide range of theoretical studies of double (e.g., Refs. 13–21) and triple (e.g., Refs. 22–29) quantum dot systems.

Motivated in part by recent experiments involving triple dot devices,^{4–7} we consider here a system of three mutually tunnel-coupled single-level quantum dots, one of which is connected to a metallic lead: a triple quantum dot (TQD) ring structure, the simplest to exhibit frustration. We focus on the TQD in the three-electron Coulomb blockade valley and study its evolution as a function of the interdot tunnel couplings, using both perturbative arguments and the full density matrix^{30,31} formulation of Wilson’s numerical renormalization group (NRG) technique^{32,33} (for a recent review, see Ref. 34). A rich range of behavior is found to occur. Both antiferromagnetic and ferromagnetic Kondo physics are shown to arise in the system—with the two distinct ground states separated by a quantum phase transition—and should be experimentally accessible via side-gate control of the tunnel couplings. The zero-bias differential conductance (G) through the dots is shown to drop discontinuously across the transition at zero temperature, from the unitarity limit of

$G/G_0=1$ in the strong coupling (SC) antiferromagnetic phase (with $G_0=2e^2/h$ as the conductance quantum) to $G/G_0=0$ in the weak coupling local moment (LM) phase. However in a certain temperature window in the vicinity of the transition, the conductance is found to be controlled by the transition fixed point (TFP) separating the two ground state phases comprising both a Kondo singlet state and a residual local moment; in particular such that *increasing* temperature in the local moment phase actually revives the antiferromagnetic Kondo effect.

II. MODELS: BARE AND EFFECTIVE

We consider three semiconducting (single-level) quantum dots, arranged in a triangular geometry as illustrated in Fig. 1. Each dot is tunnel-coupled to the others, and one of them (dot “2”) is also coupled to a metallic lead. We focus explicitly on a system tuned to mirror symmetry (see Fig. 1), and study the Anderson-type model $H=H_0+H_{\text{tri}}+H_{\text{hyb}}$. Here $H_0=\sum_{k,\sigma}\epsilon_k a_{k\sigma}^\dagger a_{k\sigma}$ refers to the noninteracting lead, which is coupled to dot 2 via $H_{\text{hyb}}=\sum_{k,\sigma}V(a_{k\sigma}^\dagger c_{2\sigma}+\text{H.c.})$, while H_{tri} describes the isolated TQD with tunnel couplings t and t' ,

$$H_{\text{tri}}=\sum_i(\epsilon_i \hat{n}_i+U \hat{n}_{i1} \hat{n}_{i2})+\sum_\sigma [t c_{2\sigma}^\dagger(c_{1\sigma}+c_{3\sigma})+t' c_{1\sigma}^\dagger c_{3\sigma}+\text{H.c.}], \quad (1)$$

where $\hat{n}_i=\sum_\sigma \hat{n}_{i\sigma}=\sum_\sigma c_{i\sigma}^\dagger c_{i\sigma}$ is the number operator for dot i . U is the intradot Coulomb repulsion and ϵ_i is the level energy of dot i , such that $\epsilon_1=\epsilon_3\equiv\epsilon$ for a mirror symmetric system

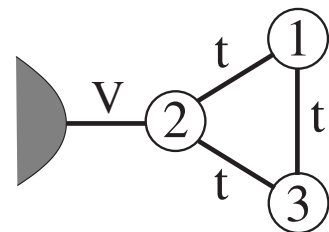


FIG. 1. Schematic illustration of the quantum dot trimer.

(in which H is invariant under a $1 \leftrightarrow 3$ permutation). For convenience we take $\epsilon_i = \epsilon$ for all dots (although this is not required, as mentioned further below).

We are interested in the TQD deep in the $\mathcal{N}=3$ electron Coulomb blockade valley. To this end, noting that coupled quantum dot experiments typically correspond to $t/U \sim 10^{-2}$,⁶ we consider the representative case $\epsilon = -U/2$ with $U \gg (t, t')$. Each dot is then in essence singly occupied, with $\mathcal{N}=2$ or 4 states much higher ($\sim \frac{1}{2}U$) in energy. The $\mathcal{N}=3$ states of the isolated TQD comprise two lowest doublets and a spin quartet (which always lies highest in energy). As the tunnel coupling t' is increased, there is a level crossing of the doublets, which are degenerate by symmetry at the point $t' = t$. Projected into the singly-occupied manifold, the doublet states are

$$|+; S^z\rangle = c_{2\sigma}^\dagger \frac{1}{\sqrt{2}} (c_{1\uparrow}^\dagger c_{3\downarrow}^\dagger + c_{3\uparrow}^\dagger c_{1\downarrow}^\dagger) |\text{vac}\rangle,$$

$$|-; S^z\rangle = \frac{\sigma}{\sqrt{6}} [c_{2\sigma}^\dagger (c_{1\uparrow}^\dagger c_{3\downarrow}^\dagger - c_{3\uparrow}^\dagger c_{1\downarrow}^\dagger) - 2c_{2-\sigma}^\dagger c_{1\sigma}^\dagger c_{3\sigma}^\dagger] |\text{vac}\rangle,$$
(2)

with $S^z = \frac{\sigma}{2}$ and $\sigma = \pm$ for spins \uparrow/\downarrow . Their energy separation is $E_\Delta = E_+ - E_- = J - J'$ with antiferromagnetic exchange couplings $J = 4t^2/U$ and $J' = 4t'^2/U$, such that the levels cross at $t' = t$ (reflecting the magnetic frustration inherent at this point). The $|-; S^z\rangle$ doublet, containing triplet configurations of spins “1” and “3,” has odd parity ($-$) under a $1 \leftrightarrow 3$ interchange while $|+; S^z\rangle$, which has singlet-locked spins “1” and “3,” and behaves in effect as a spin- $\frac{1}{2}$ carried by dot 2 alone, has even parity ($+$).

On coupling to the lead the effective model describing the system on low-energy/temperature scales is obtained by a standard Schrieffer-Wolff transformation.^{12,35} Provided the doublets are not close to degeneracy, only the lower such state need be retained in the ground-state manifold: $|-; S^z\rangle$ for $J' \ll J$ and $|+; S^z\rangle$ for $J' \gg J$. In either case a low-energy model of Kondo form arises

$$H_{\text{eff}} = J_K \hat{S} \cdot \hat{S}(0), \quad (3)$$

(potential scattering is omitted for clarity), with $\hat{S}(0)$ as the conduction-band spin density at dot 2, and \hat{S} as a spin- $\frac{1}{2}$ operator representing the appropriate doublet ($\gamma = +$ or $-$). The effective Kondo coupling is $J_{K\gamma} = 2\langle \gamma; +\frac{1}{2} | \hat{S}_2^z | \gamma; +\frac{1}{2} \rangle J_K$ with \hat{S}_2 as the spin of dot 2, where $J_K = 8\Gamma/(\pi\rho U)$ with hybridization $\Gamma = \pi V^2 \rho$ and ρ is the lead density of states. Equation (2) thus gives $J_{K-} = -\frac{1}{3}J_K$, and $J_{K+} = +J_K$. Hence, for tunnel coupling $t' \ll t$ ($J' \ll J$), a ferromagnetic spin- $\frac{1}{2}$ Kondo effect arises ($J_{K-} < 0$).²⁵ Kondo quenching of the lowest doublet is in consequence ineffective and, as temperature $T \rightarrow 0$, the spin becomes asymptotically free—the stable fixed point (FP) is the LM FP with a residual entropy $S_{\text{imp}}(T=0) = \ln 2$ ($k_B = 1$).³³ The system here is the simplest example of a “singular Fermi liquid³⁶” reflected in the nonanalyticity of leading irrelevant corrections to the fixed point.^{36,37} For $t' \gg t$ by contrast, the Kondo coupling is antiferromagnetic

($J_{K+} = +J_K > 0$), destabilizing the LM fixed point. The SC FP then controls the $T \rightarrow 0$ behavior, describing the familiar Fermi-liquid Kondo singlet ground state in which the spin is screened by the lead/conduction electrons below the characteristic Kondo scale T_K , with $T_K/\sqrt{U\Gamma} \sim \exp(-1/\rho J_{K+}) = \exp(-\pi U/8\Gamma)$.³⁸

Since the fixed points for the two stable phases are distinct, a quantum phase transition must thus occur on tuning the tunnel coupling t' through a critical value $t'_c = t$. We study it below but first outline the effective low-energy model in the vicinity of the transition. Here, as the $|\pm; S^z\rangle$ states are of course near degenerate, both doublets must thus be retained in the low-energy trimer manifold, and the unity operator for the local (dot) Hilbert space is hence:

$$\hat{1} = \sum_{S^z} (|+; S^z\rangle \langle +; S^z| + |-; S^z\rangle \langle -; S^z|) \equiv \hat{1}_+ + \hat{1}_-. \quad (4)$$

The effective low-energy model then obtained by Schrieffer-Wolff is readily shown to be

$$H_{\text{eff}}^{\text{trans}} = J_K \hat{1} \hat{S}_2 \hat{1} \cdot \hat{S}(0) + \frac{1}{2} E_\Delta (\hat{1}_+ - \hat{1}_-), \quad (5)$$

with J_K as above. The final term here refers simply to the energy difference between the two doublets. It may be written equivalently as $E_\Delta \hat{T}_z$ with a pseudospin operator

$$\hat{T}_z = \frac{1}{2} (\hat{1}_+ - \hat{1}_-), \quad (6)$$

thus defined, such that the doublets are each eigenstates of it, $\hat{T}_z |\pm; S^z\rangle = \pm \frac{1}{2} |\pm; S^z\rangle$. Considering now the first term in Eq. (5), $\hat{1} \hat{S}_2 \hat{1} \equiv \hat{1}_+ \hat{S}_2 \hat{1}_+ + \hat{1}_- \hat{S}_2 \hat{1}_-$ for the mirror symmetric case considered (cross terms vanish by symmetry). Direct evaluation of $\hat{1}_\pm \hat{S}_2 \hat{1}_\pm$ gives $\hat{1}_+ \hat{S}_2 \hat{1}_+ = \hat{S} \hat{1}_+$ ($= \hat{1}_+ \hat{S}$) and $\hat{1}_- \hat{S}_2 \hat{1}_- = -\frac{1}{3} \hat{1}_- \hat{S}$, where \hat{S} is a spin- $\frac{1}{2}$ operator for the dot Hilbert space (specifically $\hat{S}^z = \sum_{\gamma=\pm, S^z} |\gamma; S^z\rangle \langle \gamma; S^z|$ and $\hat{S}^\pm = \sum_{\gamma} |\gamma; \pm \frac{1}{2}\rangle \langle \gamma; \mp \frac{1}{2}|$).

Hence, using Eqs. (4) and (6) to express $\hat{1}_\pm = \frac{1}{2} (\hat{1} \pm 2\hat{T}_z)$ in terms of the pseudospin, the effective low-energy model is given from Eq. (5) by

$$H_{\text{eff}}^{\text{trans}} = \frac{1}{3} J_K (1 + 4\hat{T}_z) \hat{S} \cdot \hat{S}(0) + E_\Delta \hat{T}_z, \quad (7)$$

expressed as desired in terms of the spin \hat{S} and pseudospin \hat{T}_z . The term $E_\Delta \hat{T}_z$ is equivalent to a magnetic field acting on the pseudospin, favoring the $|-; S^z\rangle$ doublet for $E_\Delta > 0$ and $|+; S^z\rangle$ for $E_\Delta < 0$ such that Eq. (7) reduces, as it should, to one or other of Eq. (3) in the limit where the separation $|E_\Delta|$ is sufficiently large that only one of the doublets need be retained in the low-energy TQD manifold. Finally, note that the absence of pseudospin raising/lowering terms \hat{T}_z^\pm in $H_{\text{eff}}^{\text{trans}}$ reflects the strict $1 \leftrightarrow 3$ parity in the mirror symmetric setup (which cannot be broken by virtual hopping processes between dot 2 and the lead). This means that the Hilbert space of Eq. (7) separates exactly into spin and pseudospin sectors,

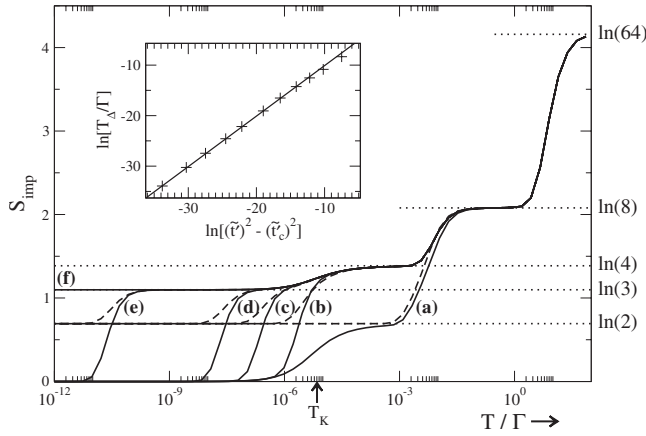


FIG. 2. Entropy $S_{\text{imp}}(T)$ vs T/Γ for fixed $\tilde{U}=10$ and $\tilde{t}=0.1$, as a function of \tilde{t}' as the transition ($\tilde{t}'_c \approx 0.097$) is approached from either side: for $t' = t'_c \pm \lambda T_K$ with $\lambda = 10^4, 10, 1, 10^{-1}, 10^{-4}$, and ≈ 0 [curves (a)–(f), respectively]. Solid lines: antiferromagnetically coupled SC phase ($\lambda > 0$); dashed lines: ferromagnetically coupled LM phase ($\lambda < 0$). Inset: close to the transition, the scale T_Δ vanishes linearly in $(\tilde{t}'^2 - t'_c{}^2)$.

such that only the *sign* of the effective Kondo coupling is correlated with the pseudospin.

III. RESULTS

The physical picture is thus clear, and indicates the presence of a quantum phase transition as a function of t' . We now present NRG results for the TQD Anderson model, using a symmetric constant lead density of states $\rho = 1/(2D)$. The full density matrix extension^{30,31} of the NRG is employed³⁴ together with direct calculation of the electron self-energy.³⁹ Calculations are typically performed for an NRG discretization parameter $\Lambda = 3$, retaining the lowest $N_s = 3000$ states per iteration.

As above we choose $\epsilon = -\frac{1}{2}U$ and $t/U = 10^{-2}$, which realistic case⁶ corresponds to single occupancy of the dots (all calculations give $\langle \hat{n}_i \rangle = 1$ for each dot). The low-temperature behavior is determined by three fixed points: those for the two stable phases at $T=0$ (SC or LM), and a “transition fixed point” precisely at the transition, which at *finite* T strongly affects the behavior of the system close to the transition.

The T dependence of the entropy $S_{\text{imp}}(T)$ (Ref. 33) provides a clear picture of the relevant fixed points. We show it in Fig. 2 for $\tilde{U} = U/\pi\Gamma = 10$ and $\tilde{t} = t/\pi\Gamma = 0.1$ (with $\Gamma/D = 10^{-2}$) for variable $\tilde{t}' = t'/\pi\Gamma$ approaching the transition from either side: $t' = t'_c \pm \lambda T_K$, varying λ . Here $\tilde{t}'_c = 0.09715\dots$ ($\approx \tilde{t}$ as expected), and the antiferromagnetic Kondo scale $T_K/\Gamma \approx 7 \times 10^{-6}$.³⁸ Solid lines refer to systems in the SC phase ($t' > t'_c$) while dashed lines refer to the LM phase ($t' < t'_c$). In all cases the highest T behavior is governed by the free orbital fixed point,³³ with all 4^3 states of the TQD thermally accessible and hence $S_{\text{imp}} = \ln(64)$. On the scale $T \sim U$ the dots become singly occupied with the entropy thus dropping to $\ln(8)$.

On further lowering T deep in either the LM or SC phases [case (a) in Fig. 2], all but the lowest trimer doublet is pro-

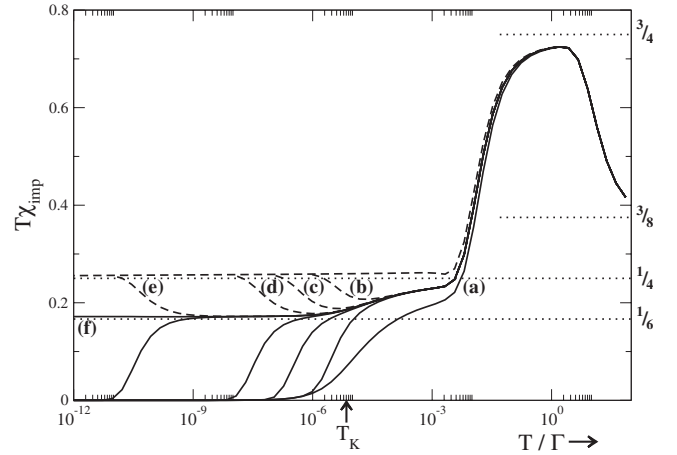


FIG. 3. Spin susceptibility $T\chi_{\text{imp}}(T)$ vs T/Γ for the same parameters as Fig. 2. Solid lines: antiferromagnetically coupled SC phase; dashed lines: ferromagnetically coupled LM phase. Close to the transition, for $|\tilde{E}_\Delta| < T < T_K$, a $T\chi_{\text{imp}}(T) = \frac{1}{6}$ plateau symptomatic of the transition fixed point arises, persisting down to $T=0$ precisely at the transition where $\tilde{E}_\Delta = 0$ [case (f)].

jected out and S_{imp} approaches $\ln(2)$, signifying the LM fixed point. For $t' < t'_c$ this remains the stable fixed point down to $T=0$ while for $t' > t'_c$ the antiferromagnetic Kondo effect drives the system to the SC fixed point below $T \sim T_K$. Lines (b)–(e) in Fig. 2 are for systems progressively approaching the transition. Here, when T exceeds the energy gap between the doublets (denoted as $|\tilde{E}_\Delta|$ and naturally renormalized slightly from the isolated TQD limit of $|E_\Delta|$), the pair of doublets are effectively degenerate⁴⁰ and an $S_{\text{imp}} = \ln(4)$ plateau is thus reached. The fixed point Hamiltonian here is then simply a free conduction band, plus two free spins [Eq. (7) with J_K and E_Δ set to zero].

For t' within $\sim T_K$ of t'_c , as in (c)–(e) of Fig. 2, a further decrease in T leads to a clear entropy plateau of $S_{\text{imp}} = \ln(3)$. This is the TFP: for $|\tilde{E}_\Delta| < T < T_K$, the $|+; S^z\rangle$ doublet is screened by the antiferromagnetic Kondo effect—even when it is *not* the ground state—while the ferromagnetically coupled $|−; S^z\rangle$ remains a local moment. The TFP thus comprises both a free local moment and a Kondo singlet, hence the $\ln(3)$ entropy. The TFP Hamiltonian corresponds to Eq. (7) with $E_\Delta = 0$, $J_K \rightarrow \infty$ in the $\mathcal{T}_z = +\frac{1}{2}$ pseudospin sector, and $J_K \rightarrow 0$ for $\mathcal{T}_z = -\frac{1}{2}$. The energy-level spectrum at the TFP thus comprises a set of LM levels plus a set of SC levels (as confirmed directly from the NRG calculations).

Finally, on a scale $T = T_\Delta \sim |\tilde{E}_\Delta|$, defined in practice by $S_{\text{imp}}(T_\Delta) = 0.85$ (suitably between $\ln 2$ and $\ln 3$), S_{imp} crosses over from the TFP value of $\ln(3)$ to the $T=0$ value appropriate to the stable fixed point (SC or LM). As the transition is approached, the scale $T_\Delta \propto (t'^2 - t'_c{}^2)$ vanishes (inset of Fig. 2)—a natural consequence of the doublet level crossing, recalling from above that $T_\Delta \approx |E_\Delta| = |J' - J| = 4|t'^2 - t^2|/U$ (with $t'_c \equiv t$ for the isolated TQD). Also since $T_\Delta = 0$ precisely at the transition, the $T=0$ entropy at that point is the TFP value $\ln(3)$, as in case (f) of Fig. 2.

The behavior described for $S_{\text{imp}}(T)$ is likewise evident in the T dependence of $T\chi_{\text{imp}}(T)$ [with $\chi_{\text{imp}}(T)$ as the total

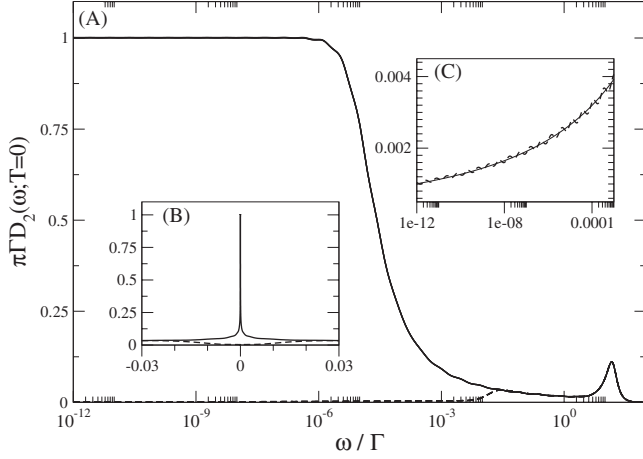


FIG. 4. $T=0$ local spectrum $\pi\Gamma D_2(\omega; T=0)$ vs ω/Γ for systems with the same parameters as Fig. 2. Panels (A) and (B) show all data on logarithmic and linear frequency scales, respectively, with solid lines again for systems in the SC phase ($t' > t'_c$) and dashed lines for the LM phase ($t' < t'_c$). Inset (C) shows the low-frequency behavior in the LM phase, fitted to a line of the form $\pi\Gamma D_2(\omega; T=0) = a/\ln^2(|\omega|/T_0)$.

impurity/dot contribution to the uniform magnetic susceptibility³³], as shown in Fig. 3. For $T \geq U$ governed by the free orbital fixed point, $T\chi_{\text{imp}}(T) \approx 3 \times \frac{1}{8}$ as expected³³ (we set $g\mu_B \equiv 1$). On the scale $T \sim U$ the dots become singly occupied but the spins are essentially uncorrelated so $T\chi_{\text{imp}}(T) \approx 3 \times \frac{1}{4}$ as expected for three free spins.³³ On further decreasing T , the ultimate low-temperature behavior is naturally $T\chi_{\text{imp}}(T) = \frac{1}{4}$ for the ground doublet characteristic of the LM phase $t' < t'_c$, and $T\chi_{\text{imp}}(T) = 0$ for the quenched SC fixed point when $t' > t'_c$. Close to the transition, however, for $|\tilde{E}_\Delta| < T < T_K$, the TFP is again evident in the persistence of a $T\chi_{\text{imp}}(T) = \frac{1}{6}$ plateau, readily understood as the mean $\langle (S^z)^2 \rangle$ for the three quasidegenerate states arising for $|\tilde{E}_\Delta| < T < T_K$ as described above, and to which value $T\chi_{\text{imp}}(T)$ tends as $T \rightarrow 0$, precisely at the transition [case (f) of Fig. 3].

Most importantly, the physics above is clearly manifest in transport properties. The zero-bias conductance through dot 2 is⁴¹

$$G(T)/G_0 = \pi\Gamma \int_{-\infty}^{\infty} -\frac{\partial f(\omega)}{\partial \omega} D_2(\omega; T) d\omega, \quad (8)$$

with $f(\omega)$ as the Fermi function and $D_2(\omega; T)$ as the local single-particle spectrum of dot 2, such that $G(T=0)/G_0 = \pi\Gamma D_2(0; 0)$. Figure 4 shows the $T=0$ spectrum for dot 2. Solid (dashed) lines are again for systems in the SC (LM) phase. At $T=0$, the $\omega=0$ spectral density collapses abruptly as the transition is crossed—from the unitarity limit of $\pi\Gamma D_2(0; 0) = 1$ in the SC phase ($t' > t'_c$) to $\pi\Gamma D_2(0; 0) = 0$ in the LM phase ($t' < t'_c$). All systems in the SC phase share a common Kondo scale so all solid lines in practice coincide and are found to be characterized by the universal scaling form obtained for the single-impurity Anderson model.⁴² In the LM phase, all $T=0$ spectra again coincide. In this case,

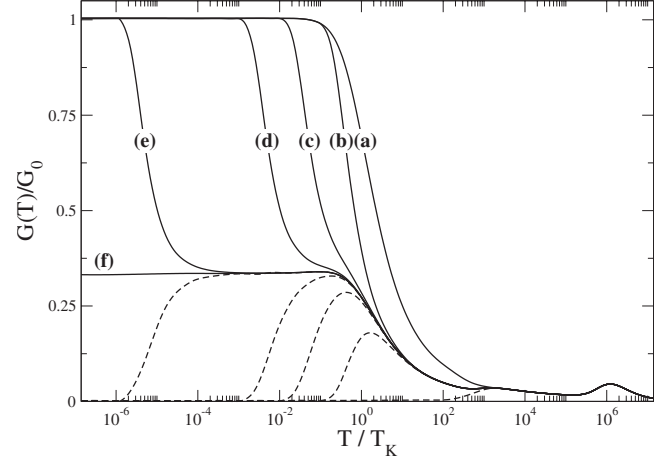


FIG. 5. Conductance $G(T)/G_0$ vs T/T_K for the same parameters as Fig. 2. As $T \rightarrow 0$, all systems in the SC phase (solid lines) satisfy the unitarity limit $G(T=0)/G_0 = 1$ while in the LM phase (dashed lines) $G(T=0)/G_0 = 0$. When $T_\Delta < T < T_K$, the conductance is controlled by the transition FP, with $G(T)/G_0 = \frac{1}{3}$ in both phases.

however, the low- ω behavior is described by $\pi\Gamma D_2(\omega; T=0) \sim a/\ln^2(|\omega|/T_0)$ (as shown in inset (C) of Fig. 4), as expected for a singular Fermi liquid,³⁷ in which the slow approach to the fixed point is characterized by marginally irrelevant logarithmic corrections.^{36,37}

The zero-bias conductance as a function of T/T_K is itself shown in Fig. 5. At $T=0$, $G(0)/G_0 = 1$ or 0 in the SC or LM phases, respectively, as above. Far from the transition [case (a)], $G(T)$ decays steadily with increasing T in the SC phase, reflecting thermal destruction of the coherent Kondo singlet. In the LM phase by contrast, $G(T)/G_0$ is not appreciable at any T . Close to the transition, however, and for $T_\Delta \leq T \leq T_K$, the transition FP controls the zero-bias conductance, and $G(T)/G_0 = \frac{1}{3}$ is seen in both SC and LM phases—meaning in particular that *warming* a system in the ferromagnetically coupled LM phase produces a revival of the *antiferromagnetic* Kondo effect. This behavior is readily understood by noting that, at $T=0$ (as in Fig. 4), $D_2(\omega; 0) \equiv D_2^{\text{LM}}(\omega)$ for $t' < t'_c$, as only excitations from the doubly degenerate LM ground states are relevant while for $t' > t'_c$, $D_2(\omega; 0) \equiv D_2^{\text{SC}}(\omega)$ since now only excitations from the Kondo singlet arise. At finite T , however, with $T_\Delta \leq T \ll T_K$ such that the lowest manifold of states comprises both the LM and the Kondo singlet, it is easy to show from the Lehmann representation of the spectrum that $D_2(\omega; T) = \frac{1}{3}[D_2^{\text{SC}}(\omega) + 2D_2^{\text{LM}}(\omega)]$ [such that $\pi\Gamma D_2(\omega; T) = 1/3$ for $|\omega| \lesssim T_K$], and hence from Eq. (8) that $G(T)/G_0 = 1/3$ —which persists down to $T=0$ precisely at the transition, where $T_\Delta = 0$ [case (f) of Fig. 5].

IV. CONCLUSION

The TQD ring system in the three-electron Coulomb blockade valley exhibits a rich range of physical behavior. Both antiferromagnetic and ferromagnetic spin- $\frac{1}{2}$ Kondo physics are accessible on tuning the tunnel coupling t' with the two phases being separated by a level crossing quantum

phase transition, reflected in a transition fixed point which controls in particular the conductance in the vicinity of the transition. We also add that, while explicit results have been given for a mirror symmetric TQD with $\epsilon_i = \epsilon$ ($= -U/2$) for all dots, our conclusions are robust provided that the dots remain in essence singly occupied. Varying ϵ (or U) on dot 2, for example, making it inequivalent to dots 1 and 3, does not break mirror symmetry and leaves unaltered the behavior uncovered above. Indeed even breaking mirror symmetry via, e.g., distinct tunnel couplings between all dots, still results in both ferromagnetically-coupled and antiferromagnetically-coupled (Kondo quenched) ground

states separated by a quantum phase transition.⁴³ The robustness of the essential physics suggests that both phases should be experimentally accessible in a TQD device, as too should the transition between them, provided the tunnel couplings can be sufficiently finely tuned.

ACKNOWLEDGMENTS

We are grateful to M. Galpin, C. Wright, and T. Kuzmenko for stimulating discussions. This research was supported in part by EPSRC-GB Grant No. EP/D050952/1.

-
- ¹D. Goldhaber-Gordon, H. Shtrikman, D. Mahalu, D. Abusch-Magder, U. Meirav, and M. A. Kastner, *Nature (London)* **391**, 156 (1998).
- ²H. Jeong, A. M. Chang, and M. R. Melloch, *Science* **293**, 2221 (2001).
- ³R. H. Blick, R. J. Haug, J. Weis, D. Pfannkuche, K. V. Klitzing, and K. Eberl, *Phys. Rev. B* **53**, 7899 (1996).
- ⁴D. Schröer, A. D. Greentree, L. Gaudreau, K. Eberl, L. C. L. Hollenberg, J. P. Kotthaus, and S. Ludwig, *Phys. Rev. B* **76**, 075306 (2007).
- ⁵A. Vidan, R. Westervelt, M. Stopa, M. Hanson, and A. Gossard, *J. Supercond.* **18**, 223 (2005).
- ⁶L. Gaudreau, S. A. Studenikin, A. S. Sachrajda, P. Zawadzki, A. Kam, J. Lapointe, M. Korkusinski, and P. Hawrylak, *Phys. Rev. Lett.* **97**, 036807 (2006).
- ⁷M. C. Rogge and R. J. Haug, *Phys. Rev. B* **77**, 193306 (2008).
- ⁸K. Grove-Rasmussen, H. I. Jørgensen, T. Hayashi, P. E. Lindelof, and T. Fujisawa, *Nano Lett.* **8**, 1055 (2008).
- ⁹T. Jamneala, V. Madhavan, and M. F. Crommie, *Phys. Rev. Lett.* **87**, 256804 (2001).
- ¹⁰T. Uchihashi, J. Zhang, J. Kröger, and R. Berndt, *Phys. Rev. B* **78**, 033402 (2008).
- ¹¹L. P. Kouwenhoven and L. I. Glazman, *Phys. World* **14**, 33 (2001).
- ¹²A. C. Hewson, *The Kondo Problem to Heavy Fermions* (Cambridge University Press, Cambridge, 1993).
- ¹³K. Kikoin and Y. Avishai, *Phys. Rev. Lett.* **86**, 2090 (2001).
- ¹⁴M. Vojta, R. Bulla, and W. Hofstetter, *Phys. Rev. B* **65**, 140405(R) (2002).
- ¹⁵L. Borda, G. Zaránd, W. Hofstetter, B. I. Halperin, and J. von Delft, *Phys. Rev. Lett.* **90**, 026602 (2003).
- ¹⁶M. R. Galpin, D. E. Logan, and H. R. Krishnamurthy, *Phys. Rev. Lett.* **94**, 186406 (2005).
- ¹⁷A. K. Mitchell, M. R. Galpin, and D. E. Logan, *Europhys. Lett.* **76**, 95 (2006).
- ¹⁸F. B. Anders, D. E. Logan, M. R. Galpin, and G. Finkelstein, *Phys. Rev. Lett.* **100**, 086809 (2008).
- ¹⁹R. López, D. Sánchez, M. Lee, M.-S. Choi, P. Simon, and K. Le Hur, *Phys. Rev. B* **71**, 115312 (2005).
- ²⁰G. Zaránd, C.-H. Chung, P. Simon, and M. Vojta, *Phys. Rev. Lett.* **97**, 166802 (2006).
- ²¹L. G. G. V. Dias da Silva, K. Ingersent, N. Sandler, and S. E. Ulloa, *Phys. Rev. B* **78**, 153304 (2008).
- ²²B. Lazarovits, P. Simon, G. Zaránd, and L. Szunyogh, *Phys. Rev. Lett.* **95**, 077202 (2005).
- ²³A. Oguri, Y. Nisikawa, and A. C. Hewson, *J. Phys. Soc. Jpn.* **74**, 2554 (2005).
- ²⁴R. Žitko, J. Bonča, A. Ramšak, and T. Rejec, *Phys. Rev. B* **73**, 153307 (2006).
- ²⁵T. Kuzmenko, K. Kikoin, and Y. Avishai, *Phys. Rev. B* **73**, 235310 (2006).
- ²⁶A. M. Lobos and A. A. Aligia, *Phys. Rev. B* **74**, 165417 (2006).
- ²⁷W. Z. Wang, *Phys. Rev. B* **76**, 115114 (2007).
- ²⁸M. Ferrero, L. D. Leo, P. Lecheminant, and M. Fabrizio, *J. Phys.: Condens. Matter* **19**, 433201 (2007).
- ²⁹F. Delgado and P. Hawrylak, *J. Phys.: Condens. Matter* **20**, 315207 (2008).
- ³⁰R. Peters, T. Pruschke, and F. B. Anders, *Phys. Rev. B* **74**, 245114 (2006).
- ³¹A. Weichselbaum and J. von Delft, *Phys. Rev. Lett.* **99**, 076402 (2007).
- ³²K. G. Wilson, *Rev. Mod. Phys.* **47**, 773 (1975).
- ³³H. R. Krishnamurthy, J. W. Wilkins, and K. G. Wilson, *Phys. Rev. B* **21**, 1003 (1980); **21**, 1044 (1980).
- ³⁴R. Bulla, T. Costi, and T. Pruschke, *Rev. Mod. Phys.* **80**, 395 (2008).
- ³⁵J. Schrieffer and P. Wolff, *Phys. Rev.* **149**, 491 (1966).
- ³⁶P. Mehta, N. Andrei, P. Coleman, L. Borda, and G. Zaránd, *Phys. Rev. B* **72**, 014430 (2005).
- ³⁷W. Koller, A. C. Hewson, and D. Meyer, *Phys. Rev. B* **72**, 045117 (2005).
- ³⁸The U dependence of T_K extracted from the numerics confirms the mapping of the full tunneling H onto a spin- $\frac{1}{2}$ Kondo model, with $T_K \propto U \sqrt{\rho J_{K+}} \exp(-1/\rho J_{K+})$ (Ref. 33) and $\rho J_{K+} = 8\Gamma/(\pi U)$ as obtained perturbatively above.
- ³⁹R. Bulla, A. C. Hewson, and T. Pruschke, *J. Phys.: Condens. Matter* **10**, 8365 (1998).
- ⁴⁰The trimer quartet state is always higher in energy, and thermally inaccessible for $T \ll \max(4t^2/U, 4t'^2/U)$.
- ⁴¹Y. Meir and N. S. Wingreen, *Phys. Rev. Lett.* **68**, 2512 (1992).
- ⁴²T. A. Costi, A. C. Hewson, and V. Zlatić, *J. Phys.: Condens. Matter* **6**, 2519 (1994).
- ⁴³Here the spin- $\frac{1}{2}$ pseudospin is not of course conserved, and the transition itself is no longer a simple level crossing.